NACA

RESEARCH MEMORANDUM

INVESTIGATION OF THE EFFECTS OF BODY CAMBER AND BODY INDENTATION ON THE LONGITUDINAL CHARACTERISTICS OF A 60° DELTA-WING—BODY COMBINATION AT A MACH NUMBER OF 1.61

By John R. Sevier, Jr.

Langley Aeronautical Laboratory
Langley Field, Va.

CLASSIFIED DOCUMENT

NATIONAL ADVISORY COMMITTEE
FOR AERONAUTICS

WASHINGTON
April 20, 1956

(CLASSIFICATION CHANGED TO Unclassified)

NASA Tech Pub Announcement #5
(AUTHORITY TO CHANGE)

26 Aug 59

RK
(GRADE OF OFFICER MAKING CHANGE)

9 March 61
DATE

H

NACA RM L56A03

NATIONAL ADVISORY COMMITTEE FOR AERONAUTICS

RESEARCH MEMORANDUM

INVESTIGATION OF THE EFFECTS OF BODY CAMBER AND BODY INDENTATION ON THE LONGITUDINAL CHARACTERISTICS OF A 60° DELTA-WING—BODY COMBINATION AT A MACH NUMBER OF 1.61

By John R. Sevier, Jr.

SUMMARY

An investigation has been made in the Langley 4- by 4-foot supersonic pressure tunnel to determine the effects of body camber and body indentation on the longitudinal characteristics of a delta-wing—body combination at a Mach number of 1.61. In combination with a 3-percent-thick 60° delta wing, the following three bodies were tested: (1) a basic parabolic body (Sears-Haack), (2) a body indented so as to have an improved wing-body area distribution at a Mach number of 1.8, and (3) a body which was both indented and cambered. In the case of the latter configuration, the effect of wing incidence was also investigated. Results indicated that neither body camber, body indentation, nor wing incidence had any appreciable effect at a Mach number of 1.61 on the minimum drag or maximum lift-drag ratios of the configurations tested. There was, however, a significant effect of body camber in displacing the pitching-moment curve in a direction favorable for the reduction of trim drag. All tests were conducted at a Mach number of 1.61 and a Reynolds number of 3.01×10^6 based on the wing mean aerodynamic chord.

INTRODUCTION

One of the key elements in attaining high lift-drag ratios is the reduction of drag due to lift. A possible approach suggested by Mr. Richard T. Whitcomb of the Langley Aeronautical Laboratory involves the use of body camber in an effort to redistribute the lift loading of a wing-body combination. Results of the first tests of this scheme in the Langley 8-foot transonic tunnel indicated that at transonic speeds there was essentially no effect on drag due to lift as a result of body cambering. There was, however, the possibility that the method would prove

more effective at supersonic speeds. For this reason, an investigation was made in the Langley 4- by 4-foot supersonic pressure tunnel of the same models tested in the Langley 8-foot transonic tunnel. The following three bodies were tested in combination with a 60° delta wing: (1) a parabolic body (Sears-Haack), (2) a body indented using the supersonic area rule (ref. 1) so as to have an improved wing-body area distribution at a Mach number of 1.8, and (3) a body which was both indented and cambered.

All tests reported herein were made at a Mach number of 1.61 and a Reynolds number of 3.01×10^6 based on the wing mean aerodynamic chord.

SYMBOLS

b	wing span
c	wing chord parallel to plane of symmetry
$\bar{c}$	wing mean aerodynamic chord, $\dfrac{\int_0^{b/2} c^2 dy}{\int_0^{b/2} c\, dy}$
i	wing incidence angle, measured from balance axis
y	spanwise distance measured from plane of symmetry
S	wing area extended through the fuselage to the center line, 0.8499 sq ft
L	lift force
D	drag force
m	pitching moment about a line perpendicular to the plane of symmetry and passing through the one-quarter chord position of the mean aerodynamic chord
q	free-stream dynamic pressure
C_L	lift coefficient, L/qS

C_D drag coefficient, D/qS

C_m pitching-moment coefficient about the one-quarter chord position of the mean aerodynamic chord, $m/qS\bar{c}$

C_{m_o} value of pitching-moment coefficient at $C_L = 0$

$C_{D_{min}}$ minimum value of drag coefficient

L/D lift-drag ratio

$(L/D)_{max}$ maximum value of lift-drag ratio

α angle of attack, measured from balance axis

θ angle of roll of model, used in obtaining area developments (Cutting plane is perpendicular to plane of symmetry at $\theta = 0^o$.)

MODELS AND TESTS

Models

Wing.- General details of the wing tested are shown in figure 1. Aspect ratio was 2.31 and thickness ratio was 0.03. An NACA 65A003 airfoil section (uncambered) was originally used in the 8-foot transonic tunnel tests, but due to leading-edge separation at the higher angles of attack, the original wing was modified by drooping the forward 1.2 inches of the airfoil as shown in figure 1(d). This modified wing proved to be effective in alleviating the separation and was therefore used for the remainder of this investigation in the 8-foot transonic and 4-foot supersonic tunnels.

Bodies.- The three bodies tested in combination with the above-described wing consisted of the following: (1) a parabolic body (Sears-Haack) of circular cross section, (2) a body indented so as to obtain an improved wing-body area distribution at a Mach number of 1.8, and (3) a body with the same indentation as (2) but which was cambered. The two indented bodies have circular cross sections over the forward part of the model, elliptical cross sections (major axis in the vertical plane) in the region of the indentation, and returned to a circular cross section near the base.

Details of the models are shown in figure 1, and area distributions are shown in figures 2 and 3. Body coordinates are given in table I and the body camber line is defined in table II. The contour of the cambered body was obtained by laying off the major axis lengths perpendicular to the camber line.

For the two uncambered body-wing combinations, a wing incidence angle of 0° was used. For the cambered body, however, since the incidence of the body in the region where the wing was attached was 5°, the wing incidence was made to be 5°, measured with respect to the balance axis. In addition, through the use of 2° wedges, an incidence angle of 3° was also tested on the cambered configuration.

Tests and Accuracy

All tests were conducted at a Mach number of 1.61 and a Reynolds number of 3.01×10^6 based on the wing mean aerodynamic chord. Tunnel stagnation pressure was 13 psia and stagnation temperature was 100° F. Dewpoint was maintained at a level where condensation effects would be negligible.

Forces and moments were measured by means of an internal strain-gage balance housed within the model. Corrections were applied to all data so that the base pressure was adjusted to free-stream static pressure.

All tests reported herein are for natural transition. Reynolds number was sufficiently high to preclude the possibility of having extensive regions of laminar flow on the model. Results of previous tests on wing-body combinations have indicated that fixing transition at these Reynolds numbers merely causes a slight increase in drag with a corresponding decrease in lift-drag ratio. For the purpose of comparing one configuration with another, however, the effect of fixing transition is believed to be negligible. From the limited investigation of reference 2, it is indicated that there is no systematic influence of fixing transition on the effectiveness of body indentation in reducing wave drag.

The maximum error in the coefficients, based on balance characteristics and repeatability of data, is believed to be the following:

C_L	± 0.004
C_D	± 0.0005
C_m	± 0.003

Mach number variation in the test section was approximately ±0.01 and the flow angle variation in the vertical and horizontal planes was approximately ±0.1°.

PRESENTATION OF RESULTS

Basic data for the configurations tested are presented in figures 4 to 6 as plots of C_L, C_D, and L/D against angle of attack, and in figure 7 where C_m is presented as a function of C_L. The data have been grouped in such a manner as to show most readily the effects of body indentation (fig. 4), body camber (fig. 5), and wing incidence angle (fig. 6). For convenience, L/D and C_D are replotted as functions of C_L in figures 8 and 9.

RESULTS AND DISCUSSION

Effects of Indentation

In figure 4 are shown the lift and drag characteristics of the basic parabolic body-wing and the uncambered indented body-wing. Wing incidence angle for both configurations was 0°. Examination of figure 4 indicates that for the particular indented body-wing tested, there was essentially no improvement in $C_{D_{min}}$ or $(L/D)_{max}$ as compared to the parabolic body-wing at the test Mach number of 1.61. Figure 8 shows that there was no change in lift coefficient for $(L/D)_{max}$ between the two configurations and figure 7 shows that the pitching-moment curve is unaffected due to indentation. Unpublished data from these same configurations from the 8-foot transonic tunnel indicate that the same results as mentioned above were obtained in the Mach number range from 0.80 to 1.15.

Effects of Body Camber

Examination of figure 5 indicates that the combined effect of body camber and changing the wing incidence angle resulted in a slight increase in minimum drag, and also a slight increase in lift-curve slope. The shift in the curves (fig. 5) is, of course, mainly due to the change in wing incidence but may be partly due to the body camber itself. Figure 8 shows that there was essentially no change in $(L/D)_{max}$ or lift coefficient for $(L/D)_{max}$. In figure 9, where C_D is replotted as a function of C_L, it can be seen that the combined effects of wing incidence and

body camber result in a small reduction in drag due to lift; for lift coefficients above 0.10, the drags of the cambered and uncambered configurations are the same. Transonic tests indicated that there was no effect of body camber on lift and drag characteristics in the Mach number range from 0.80 to 1.15.

The most significant effect of body camber in both the present tests and in the transonic tests was to displace the pitching-moment curve in such a direction as to reduce the control deflection required for trim (fig. 7) and thereby reduce the trim drag. For example, at a lift coefficient of 0.20, the pitching-moment coefficient (about the one-quarter mean aerodynamic chord) required to trim the uncambered configuration is 0.044, while for the cambered body-wing (with 3° incidence) the pitching-moment coefficient required is only 0.021 (fig. 7). Thus, the reduction in drag to be realized is the difference in drag between the two required control deflections for trim. Since the present tests are only for a wing-body combination, it is somewhat inappropriate to discuss trim drag in the absence of elevons or a horizontal tail; however, a similar shift in the pitching-moment curve due to body camber would be expected to apply to a complete airplane configuration.

Moving the moment reference axis forward or rearward of the one-quarter mean aerodynamic chord merely rotates the pitching-moment curve about the $C_L = 0$ point and does not change the increment in C_m (at a given C_L) due to body camber. Thus, the reductions in trim drag to be realized through body camber would be expected to apply at all center-of-gravity locations.

The significance of the C_{m_o} shift observed for the cambered body can also be discussed from the standpoint of increased maneuverability at supersonic speeds. Present-day aircraft designed for high altitude, high Mach number (1.6 to 2.0) operation use much of the available control deflection merely to maintain trimmed conditions leaving little margin for maneuvering. The cambered fuselage would alleviate this problem to some extent. Unpublished data which substantiate the results of the present tests have been obtained on one manufacturer's model in which the cambered body scheme was used in the form of an upswept afterbody to achieve a favorable shift in C_{m_o}. Further agreement was obtained from a second manufacturer's tests in which the cambered body scheme consisted of placing the nose section at a positive angle of incidence in order to shift C_{m_o}.

Effect of Wing Incidence

For the two incidence angles considered herein on the cambered body-wing, there was essentially no effect of wing incidence on minimum drag, lift-curve slope, or maximum lift-drag ratio (figs. 6 and 8). Although favorable shifts in C_{m_o} were exhibited by the cambered body-wing for both incidence angles tested (fig. 7), even greater shifts would have resulted with the wing at lower angles of incidence; however, due to model limitations such configurations could not be obtained in these tests. Of the two incidence angles considered, the configuration with the 3° incidence (measured from the balance axis) caused the greater shift in C_{m_o} and would therefore result in the greater reduction in trim drag.

It is recognized that negative wing incidence will cause a favorable shift in C_{m_o} for the uncambered body-wing just as the less positive wing incidence (compare the 5° and 3° cases) caused a favorable shift in C_{m_o} for the cambered body-wing. Such improvements in C_{m_o} from negative incidence on the uncambered body would need be weighed against the disadvantages of negative incidence in landing and take-off conditions. The abovementioned configurations, along with controls-deflected data should be the subject of future investigation and would need to be carried out before a final evaluation of the cambered body scheme could be made.

CONCLUDING REMARKS

An investigation has been made in the Langley 4- by 4-foot supersonic pressure tunnel to determine the effects of body camber on the longitudinal characteristics of a wing-body combination at a Mach number of 1.61. A 60° delta wing of aspect ratio 2.31 having NACA 65A003 airfoil sections was tested in combination with the following three bodies: (1) a basic parabolic body (Sears-Haack), (2) a body indented for a Mach number of 1.8, and (3) a body which was both indented and cambered.

Results indicated that body camber had a significant effect in displacing the pitching-moment curve in a direction favorable for reducing the control deflection required for trim, thereby reducing the trim drag. For the particular configurations tested at $M = 1.61$, body camber had no effect on minimum drag or maximum lift-drag ratio. A comparison of

the basic parabolic body and the uncambered indented body indicated that indentation had no effect on the longitudinal characteristics of the wing-body combination.

Langley Aeronautical Laboratory,
National Advisory Committee for Aeronautics,
Langley Field, Va., December 21, 1955.

REFERENCES

1. Whitcomb, Richard T., and Fischetti, Thomas L.: Development of a Supersonic Area Rule and an Application to the Design of a Wing-Body Combination Having High Lift-to-Drag Ratios. NACA RM L53H31a, 1953.

2. Loving, Donald L.: A Transonic Investigation of Changing Indentation Design Mach Number on the Aerodynamic Characteristics of a 45° Sweptback-Wing—Body Combination Designed for High Performance. NACA RM L55J07, 1956.

TABLE I

BODY COORDINATES

(a) Forebody

Fuselage station	Radius, in.
0	0
.5	.165
1.0	.282
1.5	.378
2.0	.460
2.5	.540
3.0	.612
3.5	.680
4.0	.743
4.5	.806
5.0	.862
5.5	.917
6.0	.969
6.5	1.015
7.0	1.062
7.5	1.106
8.0	1.150
8.5	1.187
9.0	1.222
9.5	1.257
10.0	1.290
10.5	1.320
11.0	1.350
11.5	1.380
12.0	1.405
12.5	1.430
13.0	1.452
13.5	1.475
14.0	1.492
14.5	1.510

*Major and minor axes of ellipse. Major axis is in the vertical plane.

(b) Afterbody

Fuselage station	Basic-body radius	Indented body	
		a*	b*
15.0	1.527	1.527	1.515
15.5	1.542	1.542	1.494
16.0	1.556	1.556	1.454
16.5	1.568	1.568	1.399
17.0	1.578	1.578	1.337
17.5	1.587	1.587	1.207
18.0	1.594	1.594	1.204
18.5	1.599	1.599	1.163
19.0	1.603	1.603	1.136
19.5	1.605	1.605	1.130
20.0	1.606	1.606	1.153
20.5	1.606	1.606	1.189
21.0	1.604	1.604	1.232
21.5	1.601	1.601	1.268
22.0	1.596	1.596	1.302
22.5	1.589	1.589	1.328
23.0	1.581	1.581	1.339
23.5	1.572	1.572	1.340
24.0	1.562	1.562	1.335
24.5	1.547	1.547	1.331
25.0	1.533	1.533	1.327
25.5	1.517	1.517	1.322
26.0	1.500	1.500	1.316
26.5	1.482	1.482	1.310
27.0	1.462	1.462	1.302
27.5	1.441	1.441	1.294
28.0	1.417	1.417	1.289
28.5	1.392	1.392	1.285
29.0	1.364	1.364	1.283
29.5	1.335	1.335	1.281
30.0	1.303	1.303	1.278
30.5	1.273	1.273	1.263
31.0	1.233	1.233	1.233
31.5	1.199	1.199	1.199
31.7	1.185	1.185	1.185

[redacted]

Table II

COORDINATES FOR BODY CAMBER LINE

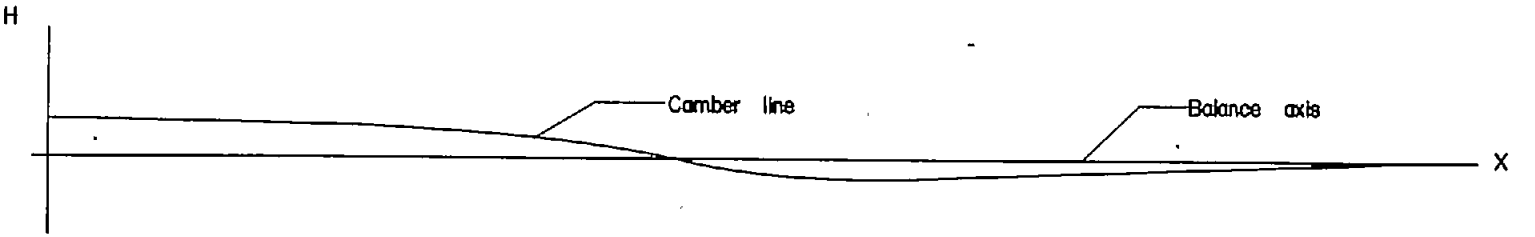

X	H
0	0.913
0.50	.904
1.00	.896
1.50	.887
2.00	.878
2.50	.869
3.00	.861
3.50	.852
4.00	.843
4.50	.834
5.00	.826
5.50	.817
6.00	.808
6.50	.800
7.00	.791
7.50	.781
8.00	.767
8.50	.747
9.00	.726
9.50	.697
10.00	.661

X	H
10.50	0,670
11.00	.570
11.50	.520
12.00	.463
12.50	.400
13.00	.327
13.50	.250
14.00	.170
14.50	.080
15.00	-.015
15.50	-.113
16.00	-.208
16.50	-.288
17.00	-.353
17.50	-.396
18.00	-.422
18.50	-.434
19.00	-.437
19.50	-.426
20.00	-.409

X	H
20.50	-0.391
21.00	-.374
21.50	-.356
22.00	-.339
22.50	-.321
23.00	-.304
23.50	-.286
24.00	-.269
24.50	-.251
25.00	-.234
25.50	-.216
26.00	-.199
26.50	-.182
27.00	-.164
27.50	-.147
28.00	-.129
28.50	-.112
29.00	-.094
29.50	-.077
30.00	-.059
30.50	-.042
31.00	-.024
31.50	-.007
31.70	0

(a) Basic body-wing.

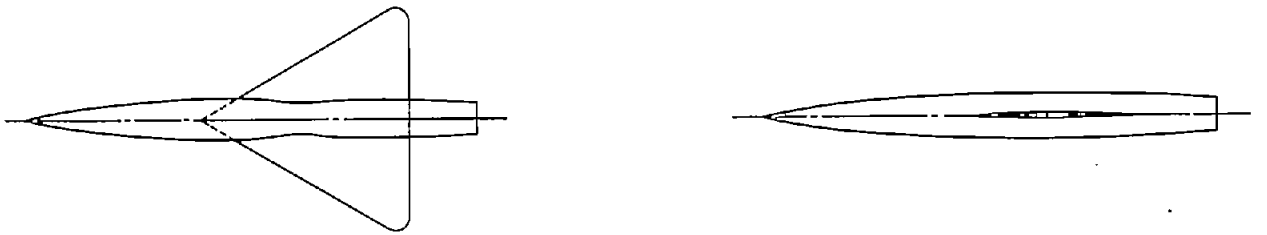

(b) Indented body-wing.

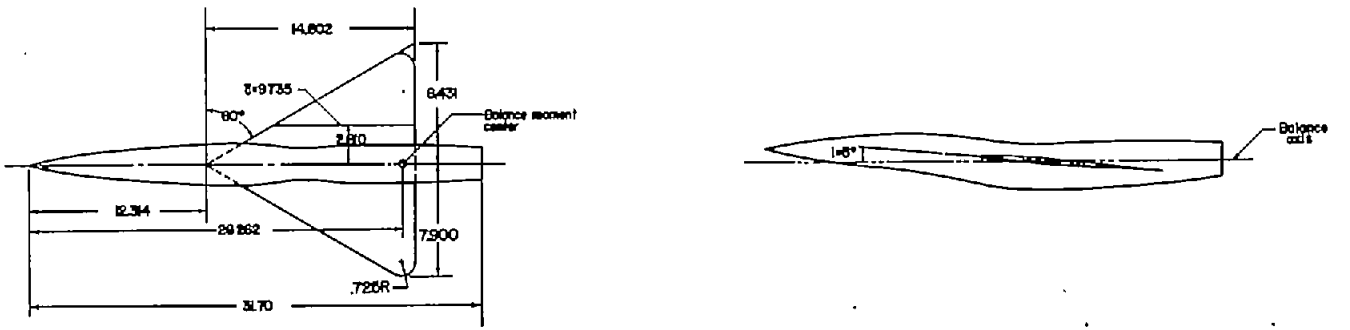

(c) Cambered and indented body-wing.

Figure 1.- General details of the models. All demensions are in inches.

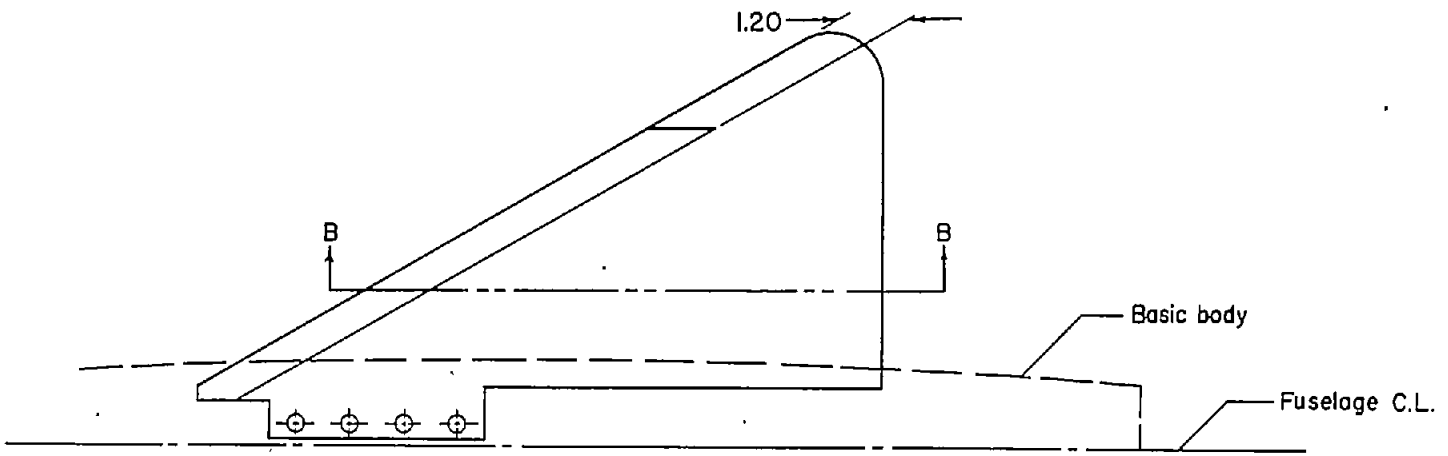

Coordinates for camber line at all spanwise stations

X	Y
0	-.053
.30	-.024
.60	-.010
.90	-.005
1.20 to T.E.	0

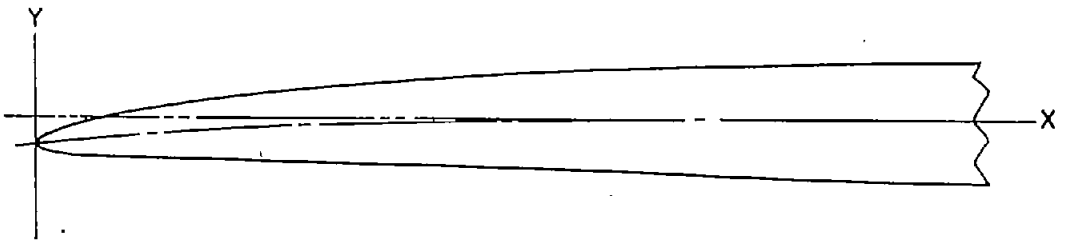

Enlarged detail of drooped leading edge at B-B

(d) Detail of wing.

Figure 1.- Concluded.

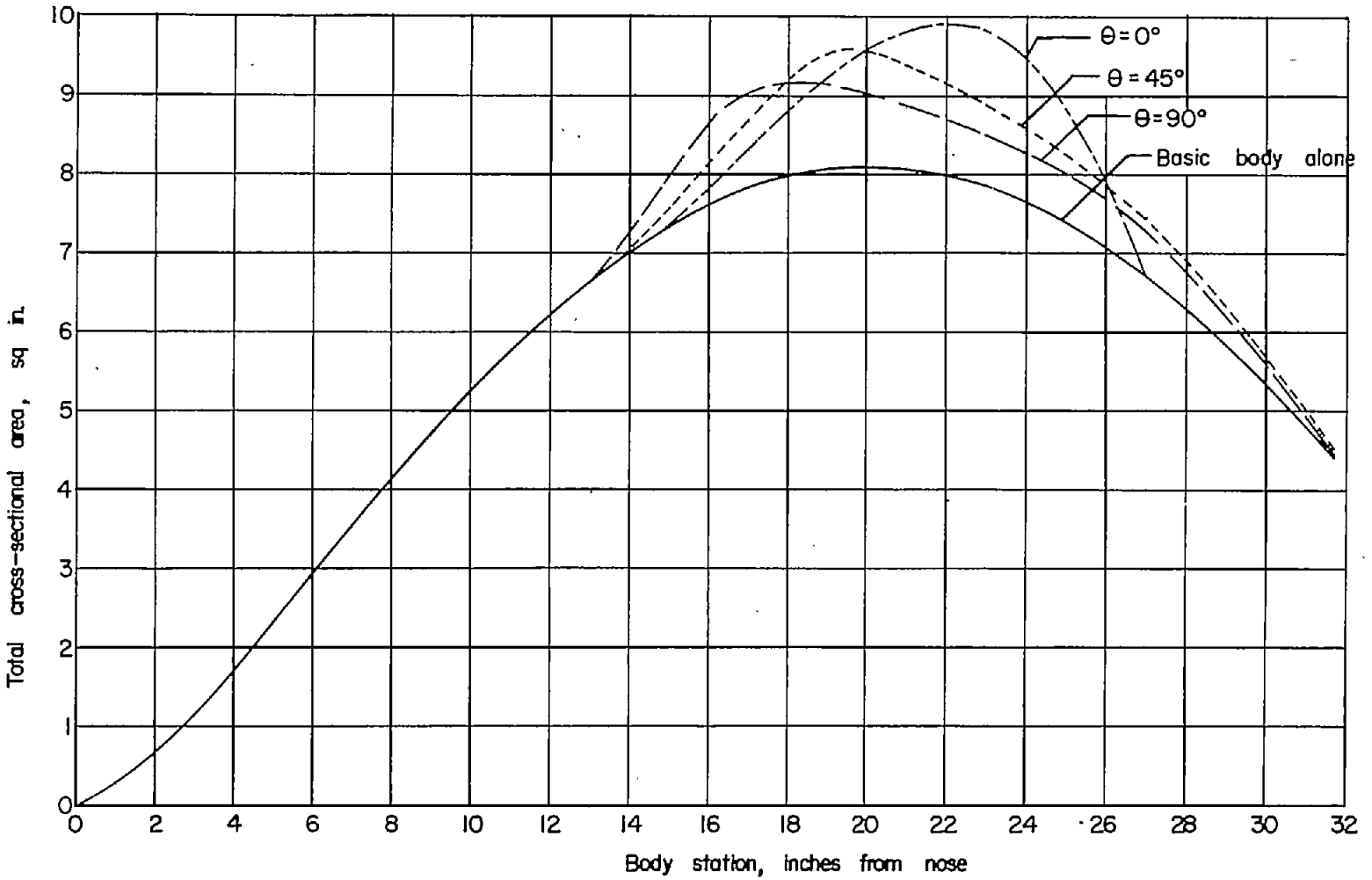

Figure 2.- Axial distribution of cross-sectional area for the basic body alone and for the basic body-wing at a Mach number of 1.6 for different roll angles.

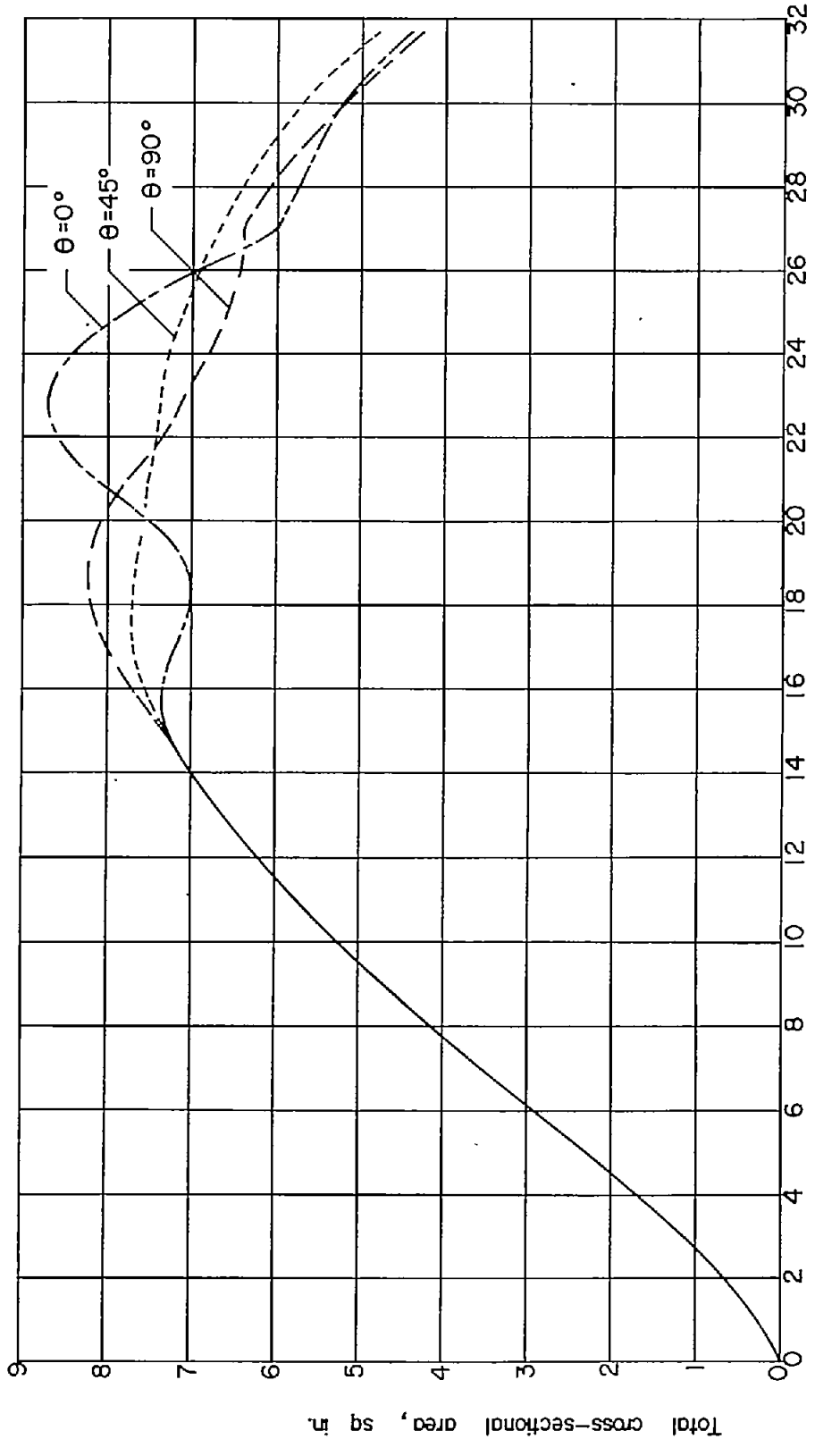

Figure 3.- Axial distribution of cross-sectional area for the indented body-wing at a Mach number of 1.6 for different roll angles.

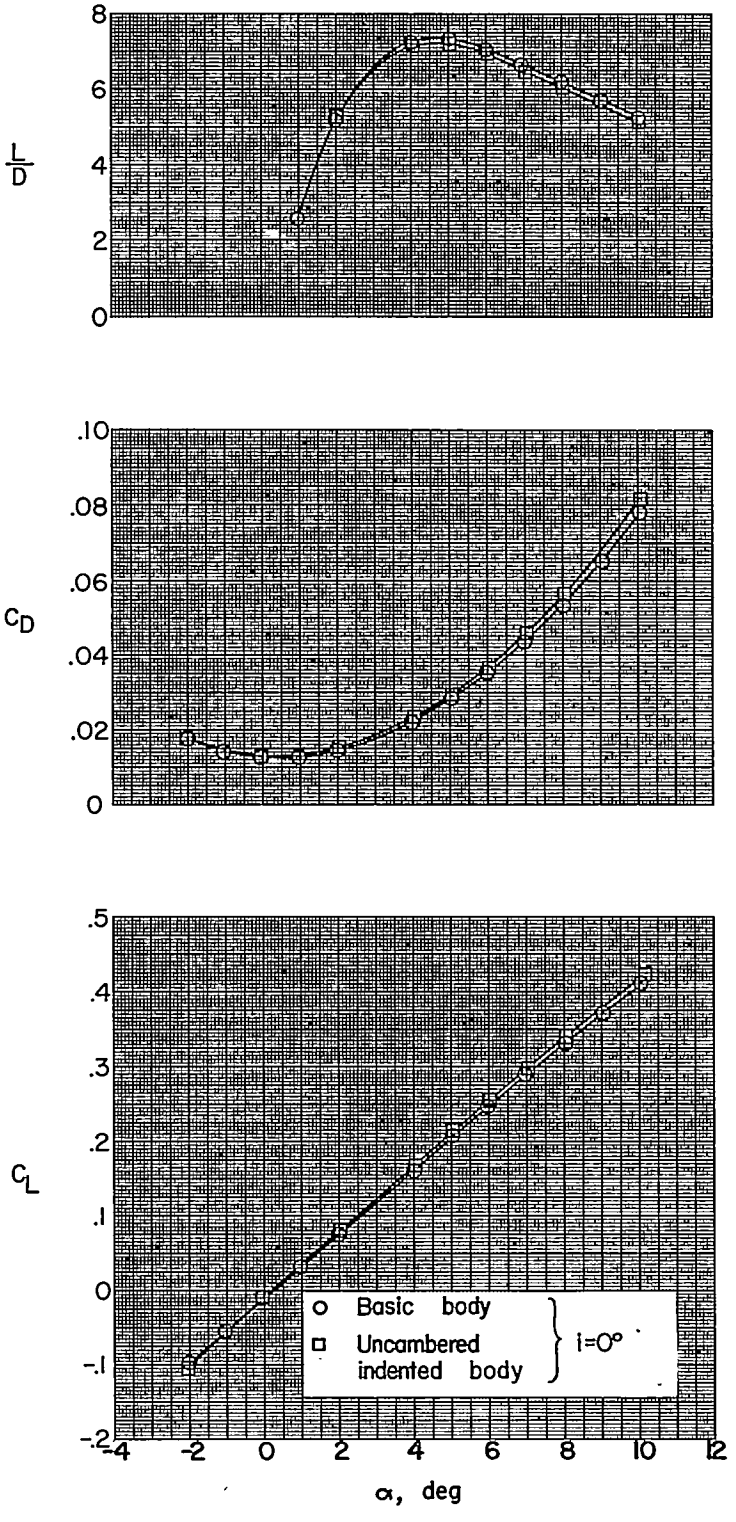

Figure 4.- Effect of body indentation on the lift and drag characteristics at M = 1.61.

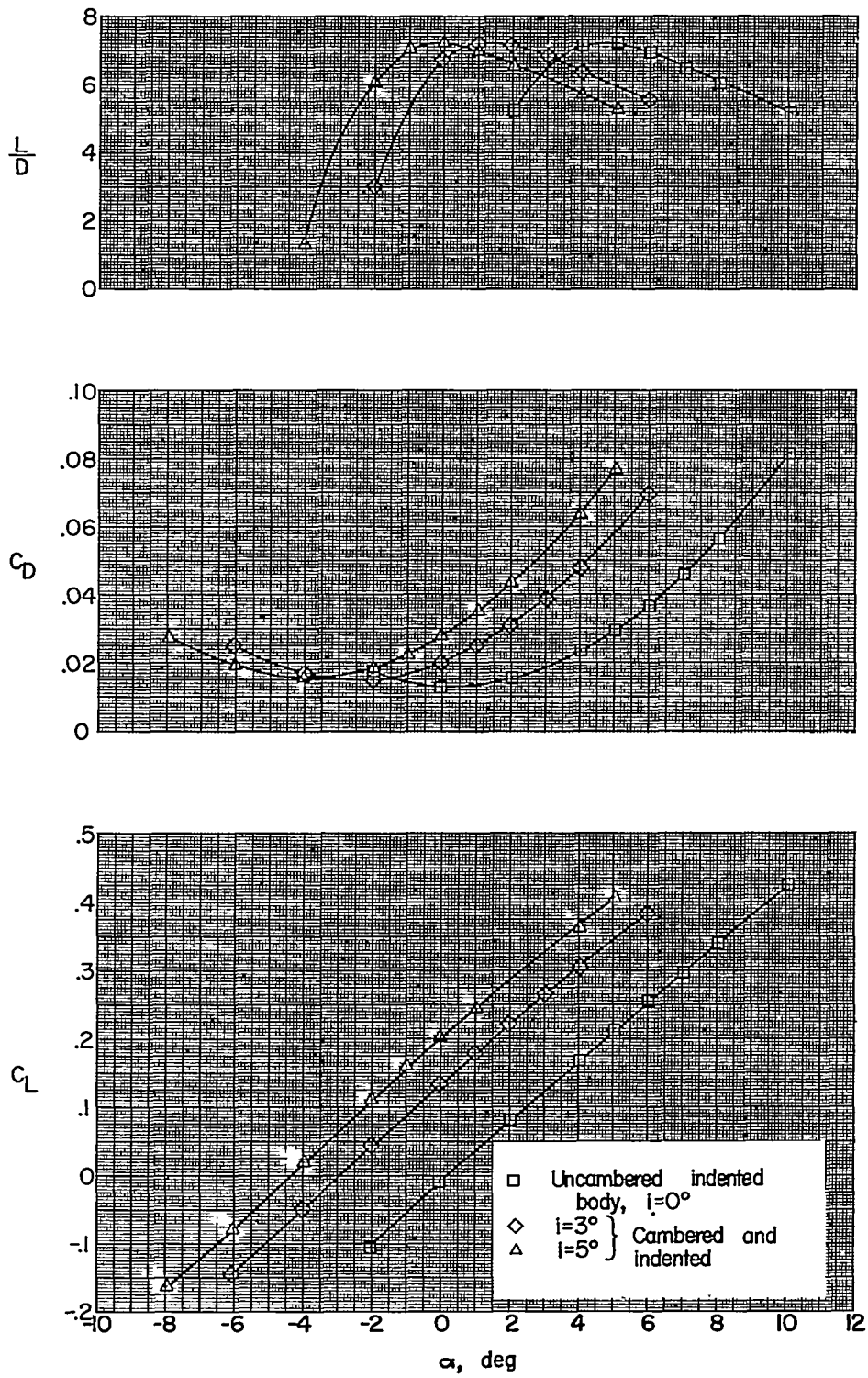

Figure 5.- Effect of body camber on the lift and drag characteristics of the various wing-body configurations at M = 1.61.

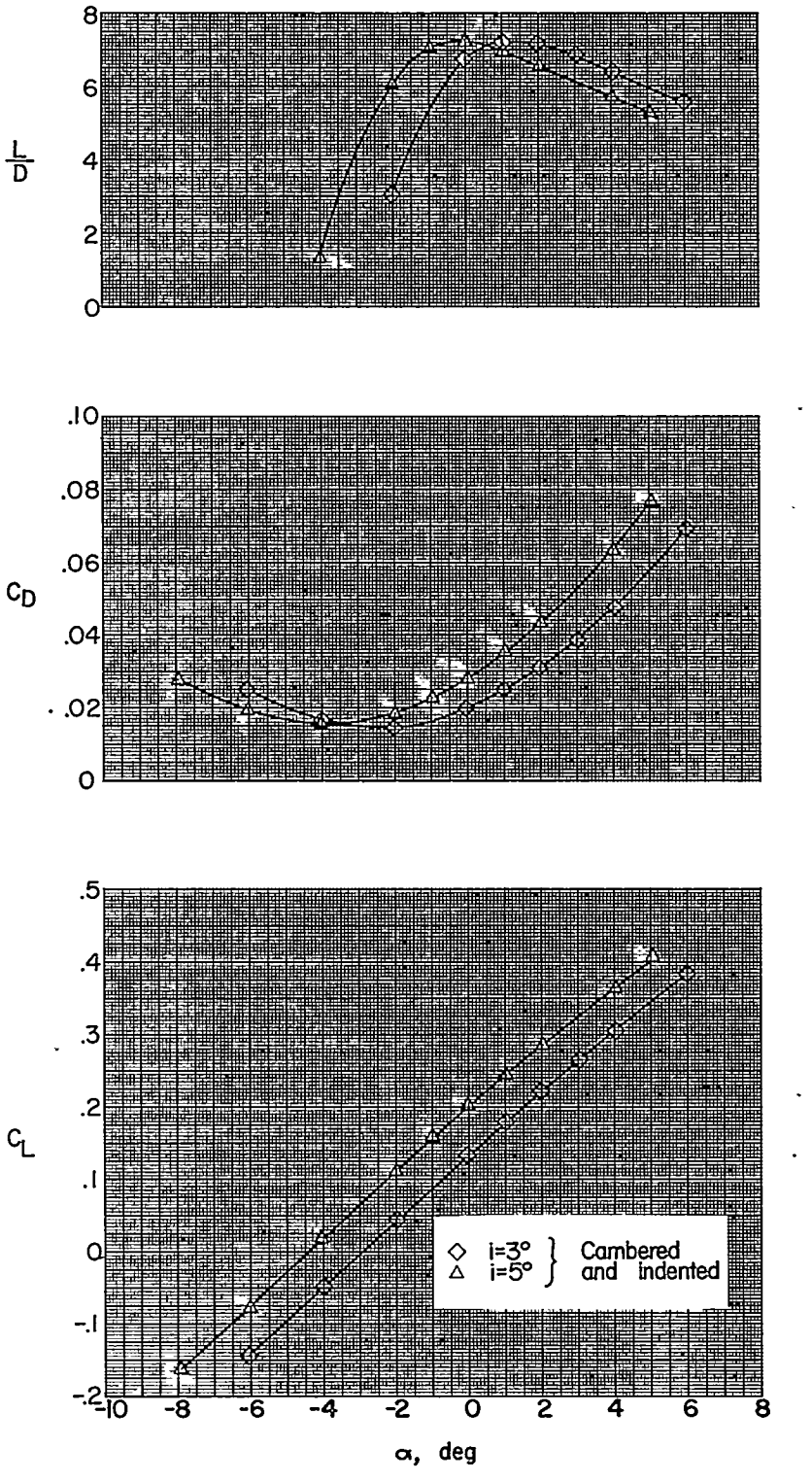

Figure 6.- Effect of wing incidence on the lift and drag characteristics at M = 1.61.

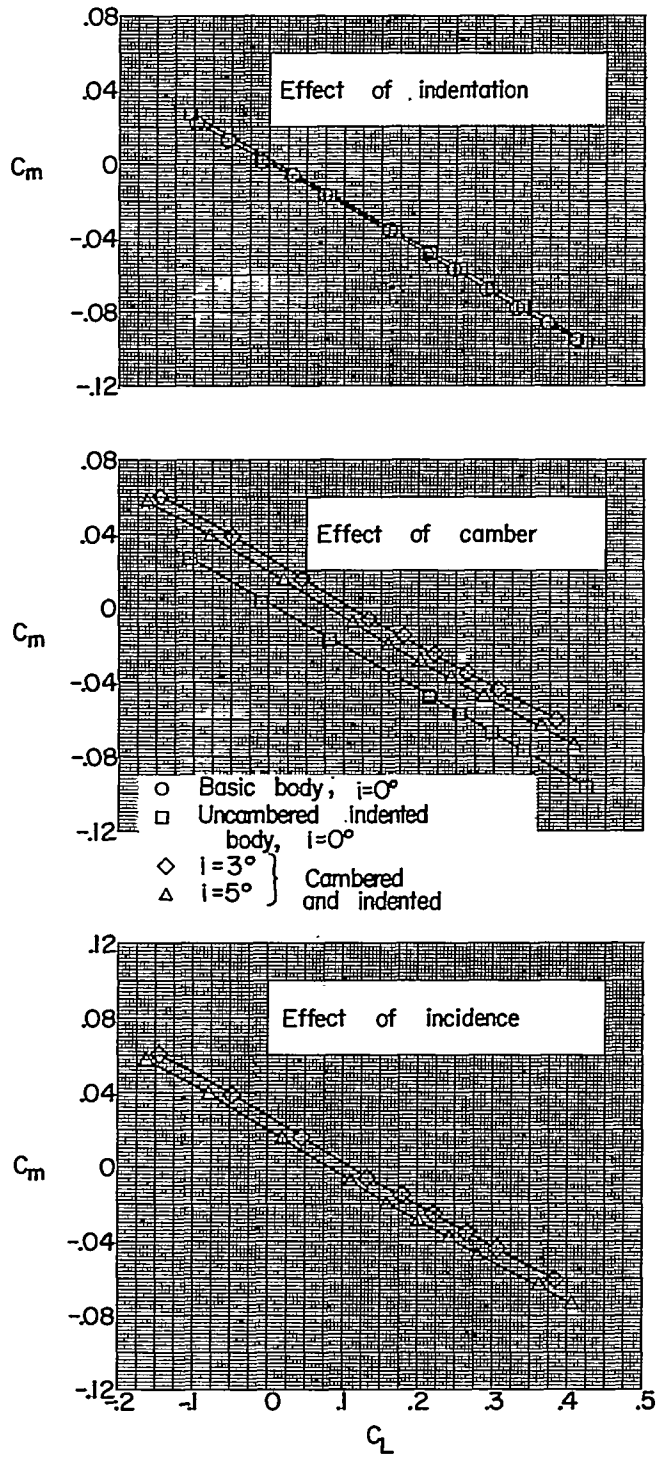

Figure 7.- Pitching-moment characteristics of the configurations tested at M = 1.61.

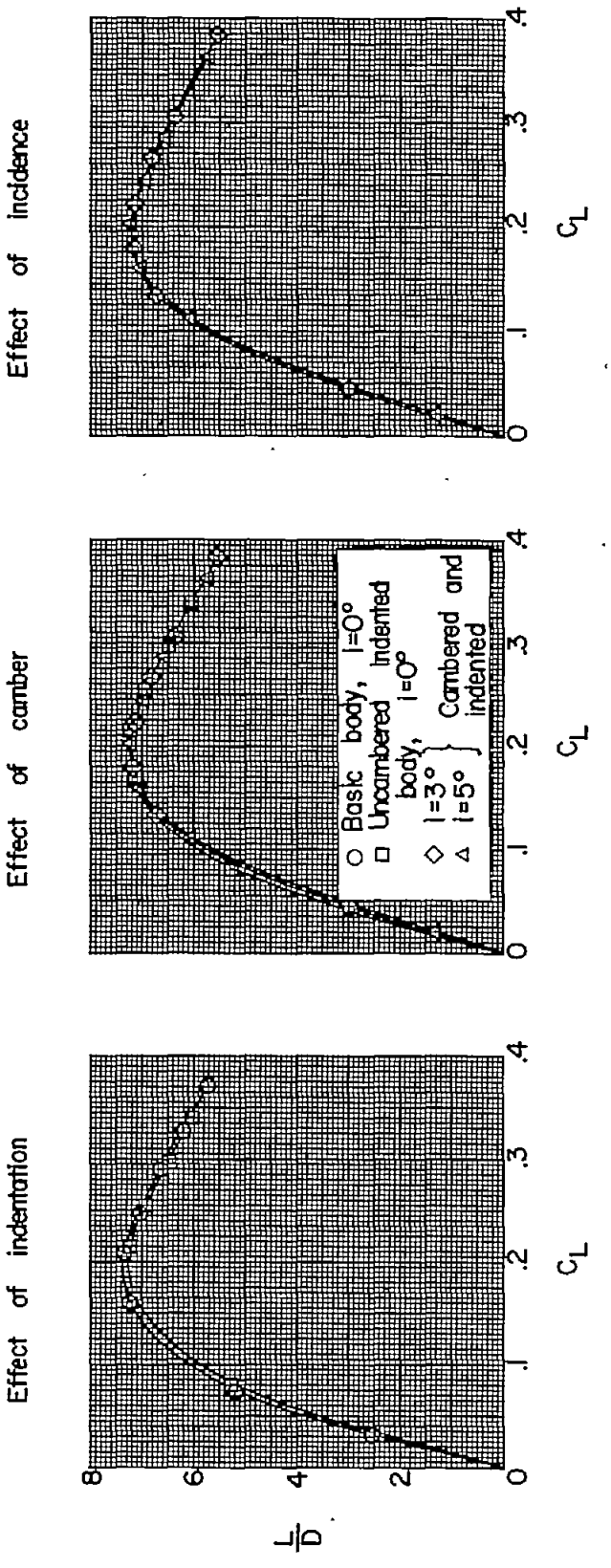

Figure 8.- Lift-drag ratios of the various configurations tested at M = 1.61.

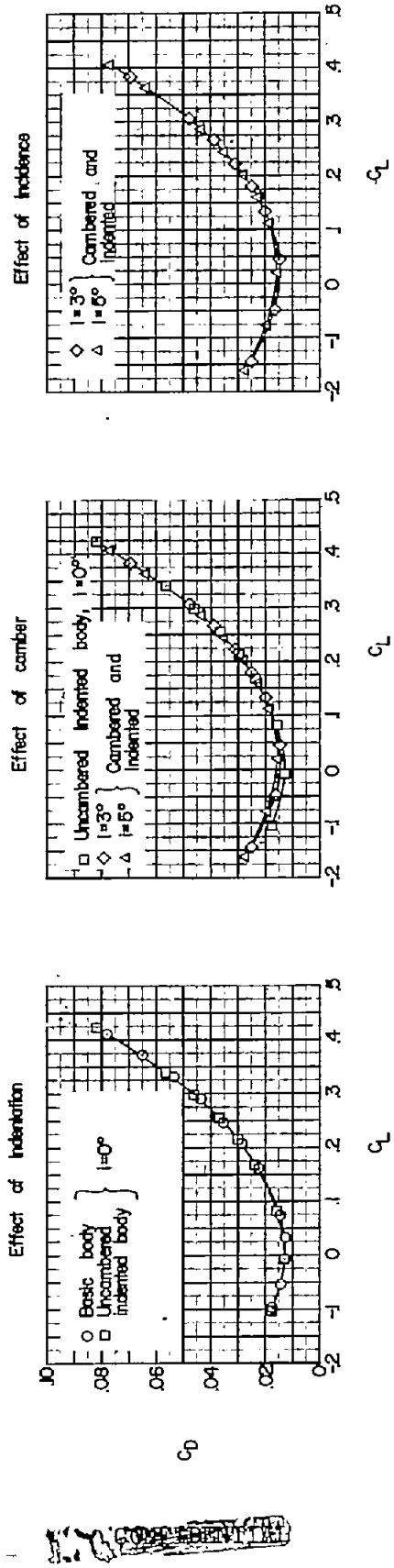

Figure 9.- Variation of drag coefficient with lift coefficient for all the configurations tested. M = 1.61.